



Microplastics in bloom-forming macroalgae: Distribution, characteristics and impacts



Zhihua Feng^{a,e,g,*}, Tao Zhang^{a,e,g}, Huahong Shi^c, Kunshan Gao^b, Wei Huang^d, Juntian Xu^{a,e,g}, Jiakuan Wang^a, Rui Wang^a, Ji Li^f, Guang Gao^{a,b,*}

^a Jiangsu Key Laboratory of Marine Bioresources and Environment, Jiangsu Ocean University, Lianyungang 222005, China

^b State Key Laboratory of Marine Environmental Science & College of Ocean and Earth Sciences, Xiamen University, Xiamen 361005, China

^c State key Laboratory of Estuarine and Coastal Research, East China Normal University, Shanghai 200241, China

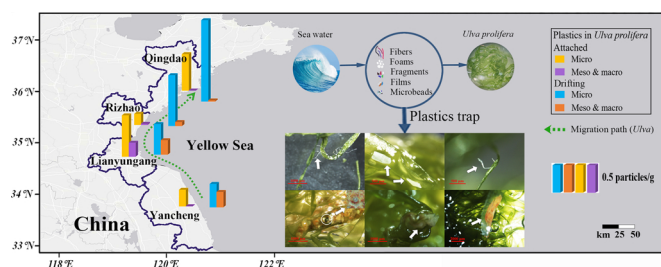
^d Key Laboratory of Marine Ecosystem and Biogeochemistry, Second Institute of Oceanography, Ministry of Natural Resources, Hangzhou 310012, China

^e Co-Innovation Center of Jiangsu Marine Bio-industry Technology, Jiangsu Ocean University, Lianyungang 222005, China

^f School of Oceanography, Shanghai Jiao Tong University, Shanghai 200030, China

^g Jiangsu Key Laboratory of Marine Biotechnology, Jiangsu Ocean University, Lianyungang 222005, China

GRAPHICAL ABSTRACT



ARTICLE INFO

Editor: Dr. R Teresa.

Keywords:

Green tides
Macroalgae
Microplastics
Photosynthesis
Ulva
Yellow Sea

ABSTRACT

Macroalgal blooms and marine microplastics (MPs), as global challenges for oceans, are both showing a rising trend. However, none is known regarding the interaction of these two important issues. The Yellow Sea suffers the world's largest green tides and severe MPs pollution as well. Therefore, we tracked the trapping of MPs by drifting *Ulva prolifera* in the Yellow Sea during the green-tide period. The abundance of MPs in drifting *U. prolifera* was 595–3917 times higher than that in seawater and increased along the drifting path from south to north in the Yellow Sea. In addition, four mechanisms of trapping plastics (twining, attachment, embedding, and wrapping) on or in *U. prolifera* were unmasked, which explains why the plant has such strong capacity to trap MPs. Laboratory incubation experiments showed that MPs ($0.025\text{--}25\text{ mg L}^{-1}$) did not affect growth rate, effective photochemical efficiency of photosystem II (PSII), or saturating irradiance of *U. prolifera* until reaching an extremely high concentration (100 mg L^{-1}), indicating a high tolerance to MPs. Due to tremendous biomass and coverage of the green tide and increased frequency as well, the plastics trap in drifting macroalgae can alter the spatio-temporal distribution of MPs in the oceans.

* Corresponding authors at: Jiangsu Key Laboratory of Marine Bioresources and Environment, Jiangsu Ocean University, Lianyungang 222005, China; State Key Laboratory of Marine Environmental Science & College of Ocean and Earth Sciences, Xiamen University, Xiamen 361005, China

E-mail addresses: fengzhihua@jou.edu.cn (Z. Feng), guang.gao@xmu.edu.cn (G. Gao).

<https://doi.org/10.1016/j.jhazmat.2020.122752>

Received 7 February 2020; Received in revised form 13 April 2020; Accepted 13 April 2020

Available online 19 April 2020

0304-3894/ © 2020 Elsevier B.V. All rights reserved.

1. Introduction

The annual production of plastics in the world has grown from 1.7 million tons in 1950 to an exceeded estimate of 335 million tons in 2016 (Plastics Europe, 2018). It has been reported that 4.8–12.7 million tons of plastics have entered the ocean and formed marine debris, accounting for 60–80 % of marine litters (Jambeck et al., 2015). Among plastics, those less than 5 mm in size are defined as microplastics (MPs) (Thompson et al., 2004). Compared to large plastics, MPs may have a wider impact on the oceans and ecosystems because MPs are easier to be dispersed throughout the oceans due to its smaller particle size. Marine MPs can release plastic additive into the environment, representing an ecotoxicological risk for marine organisms (Hermabessiere et al., 2017). As a result, marine MPs have put potential pressure on the biotic and abiotic environments (Galloway et al., 2017; Haward, 2018; Hermabessiere et al., 2017). In addition, weight concentrations (mg/L) of pelagic MPs are predicted to increase approximately fourfold by 2060 from the condition in 2016 (Isobe et al., 2019).

To date, most studies on MPs accumulation in marine organisms focus on heterotrophic organisms (Wang et al., 2019b, 2019a), and little is known on the status of MPs accumulation in autotrophic organisms, particularly for macroalgae, although MPs in nori has been reported recently (Li et al., 2020). Macroalgae provide important ecological services in coastal areas, such as sediment stabilization and providing habitats for epifauna and infauna (Gao et al., 2018; Reed et al., 2016). Furthermore, they also serve as animal feed and human food (Gao et al., 2018b), implying that MPs in or on macroalgae can be transmitted to animals and humans via food web. Macroalgae are mainly attached to rocks or other substrates. Meanwhile, there are also drifting macroalgae and some of them form large scale of blooms known as golden tides or green tides (Smetacek and Zingone, 2013). *Ulva* is a ubiquitous genus and *Ulva*-triggered green tides can occur in nearly every corner of the planet (Arroyo and Bonsdorff, 2016). Although non-toxic to humans, macroalgae blooms harm shore-based activities by virtue of their sheer physical mass. During their decomposition, the generated toxic hydrogen sulfide (H₂S) is detrimental to many organisms and services of coastal ecosystems (Arroyo and Bonsdorff, 2016; Van Alstyne et al., 2015). Due to the combination of eutrophication and climate change, these macroalgal blooms appear to increase (Gao et al., 2017a; Smetacek and Zingone, 2013; Xu et al., 2017).

Oceans are considered the endpoint of plastic fluxes from hydrological catchments (Lebreton et al., 2017). In addition, direct inputs by coastal population and industrial activity in the seas, such as commercial fishing and macriculture, also contributes to MPs abundance in oceans (Feng et al., 2020; Lusher et al., 2015). All of these lead to the MPs pollution in the oceans. Some studies have been conducted to remove MPs from wastewater before they are discharged (Enfrin et al., 2019; Yang et al., 2019). However, little is known how to remove MPs that already exist in the oceans. The ability of macroalgae to uptake nutrients and heavy metals for the remediation of contaminated environment has been verified (He et al., 2008; Murphy et al., 2007; Oberholster et al., 2014). In China, the Yellow Sea is seriously polluted by MPs (Feng et al., 2019, 2020; Zhu et al., 2018). In addition, macroalgal bloom caused by *U. prolifera* have occurred annually in the Yellow Sea since 2007, with a maximal distribution area reaching nearly 60,000 km² and approximately 20 million tonnes of biomass (Gao et al., 2010; Ye et al., 2011; Zhang et al., 2019b). Small-scale drifting *Ulva* species initially occur in the Jiangsu coast, migrate northward along the coast of the southern Yellow Sea driven by monsoons and ocean currents, accumulate and decline in the nearshore waters of the Shandong Peninsula (Zhang et al., 2019b). Based on the fact above, the Yellow Sea is an ideal area to study the interaction of MPs and macroalgal blooms. In this study, we hypothesized that bloom-forming *Ulva* species can trap and transport MPs effectively, and be thus an ideal material to treat MPs in the seas. To test this hypothesis, we investigated the MPs in drifting green macroalga *U. prolifera* in the

Yellow Sea, explored the characteristics and mechanisms of plastics trapped in *U. prolifera* during the period of green tides, and finally studied the tolerance of *U. prolifera* to high levels of MPs because high tolerance to pollutant is essential for a qualified bioremediator (Siripornadulsil and Siripornadulsil, 2013; Solovchenko and Khozin-Goldberg, 2013). This study could also provide insight into how simultaneously proceeding two global challenges—marine MPs and green tides—interact with each other.

2. Materials and methods

2.1. Sample collection and preparation

Drifting and attached *U. prolifera* were collected at 31 stations in the coastal waters of four areas (Yancheng, Lianyungang, Rizhao and Qingdao), covering the whole migration path (from south to north) of green tides occurring annually in the Yellow Sea (Liu et al., 2013; Zhang et al., 2019b). Therefore, the investigation of plastics in *U. prolifera* from these four areas helps understand the features of plastics trapping and transport by *U. prolifera* along the migration path. In addition, attached *U. prolifera* was collected at stations away from serious industrial pollution and representing the common MPs contamination conditions in the coastal zone. Four cruises, one for each area, were conducted from south to north of the Yellow Sea along the migration path (from Yancheng to Qingdao) to track the development of the green tide from April 16 to July 23 in 2018. Drifting *U. prolifera* was collected with a metal scoop net from 21 stations from F1 to F21 (Fig. 1 and Table S1). At the same time, the attached *U. prolifera* samples were collected on the coastal rocks with a metal scissor at 10 stations from A1 to A10 (Fig. 1 and Table S1). Sampling was conducted in triplicate at each station and about 200 g thalli were collected for each sampling. Following sampling, thalli of *U. prolifera* were quickly sealed with aluminum foil bags and transferred in a cooler (−5 °C) to the laboratory where they were stored at −20 °C pending processing and analysis. All samples were stored for 1–2 weeks before digestion. About 30 L of surface seawater at each station (stations for attached and drifting thalli were defined as nearshore and offshore respectively) was sampled at a 30 cm water depth in triplicate by Niskin water sampler and filtered through a 33 μm steel sieve to measure MPs abundance in seawater (Zhu et al., 2018). The particles on the steel sieve were washed into a clean glass bottle with filtered deionized water and stored pending analysis.

2.2. Quality control and assurance

The metal scoop net was used to minimize the plastics contamination from sampling tools. After sampling, the *U. prolifera* samples were quickly loaded into the aluminum foil bags to reduce the atmospheric contamination. Because MPs are ubiquitous in indoor environments (Gasperi et al., 2018), suitable preventive measures were taken to avoid or reduce plastic contamination in the laboratory. Air circulation between indoors and outdoors and the number of operators in the laboratory were minimized. The hands and forearms of operators were scrubbed three times before operation and operators were asked to wear white cotton lab coats, disposable latex gloves and face masks throughout the sample manipulation and processing. All instruments and equipment were thoroughly cleaned with 75 % alcohol and all chemical reagents and deionized water were filtered with 2.7 μm glass microfiber (Whatman Grade GF/D) before use. Solution preparation, sample digestion and observation of plastics and mechanisms of plastics trap were always conducted in a laminar flow cabinet (SW-CJ-2F, SUJING, China). Sample digestion was conducted in 12 batches and each batch included 555.00–1299.91 g samples from 2 to 4 stations. Five procedural blanks without *U. prolifera* samples were made during every batch of sample processing to determine the extent of MPs contamination under laboratory conditions.

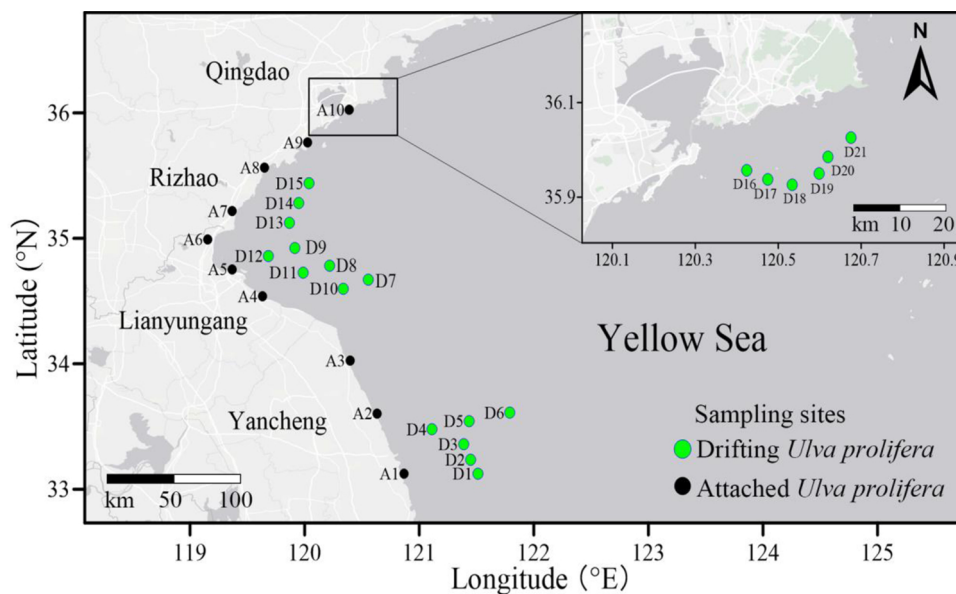


Fig. 1. Sampling stations for drifting and attached *U. prolifera* in the Yellow Sea (For interpretation of the references to colour in this figure legend, the reader is referred to the web version of this article).

2.3. Sample digestion

The surface seawater of the *U. prolifera* was removed by absorbent paper gently, and the fresh weight of *U. prolifera* was determined by a precision electronic balance (BS124S, Sartorius, Beijing) that has a closed chamber and minimizes the water loss from thalli. *U. prolifera* samples (80–120 g fresh weight) were immediately placed into a 1000 mL clean beaker and digested by 100–120 mL Fenton's reagent containing 30 % (v/v) H_2O_2 and catalyst solution (20 g of $\text{FeSO}_4 \cdot 7\text{H}_2\text{O}$ in 1 L of filtered RO water) in oscillation incubators (DKZ-3, Shanghai Yiheng, China) at 40 °C with 60 rpm for 24–48 h according to the previous studies (Fenton, 1894; Hurley et al., 2018; Tagg et al., 2017). When the solution was clear and yellow, the digestion was considered completed. The digestion solution was then transferred and filtered through 2.7 μm glass microfiber (Whatman Grade GF/D) using a filtration unit with one Büchner funnel (AP-01 P, Autoscience, China). And then, the filter membranes were placed in clean petri dishes with lids and dried at room temperature for further study.

2.4. Identification of plastics

Nikon SMZ 1500 N (Japan) stereo microscope with charge-coupled device (CCD) camera was used to isolate, photograph and measure plastics at the largest cross section and categorize according to their size, shape and colour. These parameters present important features of MPs (Auta et al., 2017; Pan et al., 2019; Veerasingam et al., 2016). In this study, micro-, meso- and macroplastics were defined as plastic particles with the size ≤ 5 mm, the size > 5 mm and ≤ 25 mm, and the size > 25 mm, respectively. MPs were classified into five shapes including microbead, film, fragment, foam and fiber, and five colour categories covering white-transparent, black-grey, blue-green, red-pink and orange-yellow. Due to the large number of potential plastic particles found (7932 particles), approximately 20 % (1561 particles) of the total filtered filters in each station were randomly selected and the plastics were identified by a micro-Fourier Transformed Infrared Spectroscopy (μ -FT-IR) (Nicolet iN10, Thermo Fisher Scientific, USA). The transmittance mode was used to measure MPs. The spectrum range was set from 650 to 4000 cm^{-1} with 64 co-scans at a resolution of 8 cm^{-1} , and the aperture ranged from 50 \times 50 mm to 150 \times 150 mm depended on the size of particles. The OMNIC software was used for the identification of polymer by comparing the samples with libraries of

standard spectra. Polymers matching with reference spectra more than 70 % were validated (Thompson et al., 2004; Cai et al., 2019). All data used to assess abundance, size and shape were based on visual identification, and μ -FT-IR was used to identify polymer composition.

2.5. Observation on the mechanisms of trapping plastics

After defrosting, about 90–120 g *U. prolifera* samples from each sampling station were randomly selected to study the microscopic trapping mechanisms of plastics in *U. prolifera* using Nikon SMZ 1500 N (Japan) stereo microscope with charge-coupled device (CCD) camera. All observed potential plastics were also isolated and identified with a μ -FT-IR (Nicolet iN10, Thermo Fisher Scientific, USA).

2.6. Growth and photosynthetic performance of *U. prolifera* exposed to MPs

Laboratory experiments were conducted to investigate the impacts of MPs on physiological performance of *U. prolifera* and the tolerance of this plant to high concentrations of MPs. To minimize the extra MPs contamination, spores, released from the fertile thalli of *U. prolifera*, were cultured and developed with filtered (0.22 μm) and autoclaved natural seawater (Gao et al., 2018a). Healthy thalli that were identified by green colour and came from the spores were used in this study. Thalli (~ 3 cm in length) were cultured at a density of 0.2 g/L in 500 mL flasks in an illuminated incubator (GXZ-500B, Ningbo, China) at 20 °C, with the illumination intensity of 300 $\mu\text{mol photons m}^{-2}\text{s}^{-1}$ (12 L:12D). Filtered (0.22 μm) and sterilized natural seawater (salinity 30, enriched with 60 mM NaNO_3 and 8 mM NaH_2PO_4) was used as culture medium. Virgin white high-density polyethylene (HDPE) particles (Huachuang Plastic Material Corporation, China) that had the highest abundance in *U. prolifera* based on field investigation were used as representative MPs. Its size distribution (range = 1.45–52.48 μm , $d_{0.5} = 18.34$ μm , $d_{0.1} = 7.78$ μm , $d_{0.9} = 36.24$ μm , specific surface area = 0.83 m^2/g , Fig. S1a) was measured using laser diffraction-based particle size analyzer (LDSA; Mastersizer 2000, Malvern instruments Ltd., UK). The microscopic and crystalline structure of HDPE particles were analyzed by Scanning electron microscope (SEM; Quanta FEG 450, FEI Ltd., USA) and X-ray diffractometer (XRD; D8 Advance, Bruker, Germany). Fig. S1 (b and c) indicated the SEM images (fragments not spheres) and XRD diffraction patterns of the HDPE particles. In addition, the polymer type was confirmed by μ -FT-IR (Fig. S1d). The HDPE

particles were added to the algal cultures to achieve the concentrations of 0.025, 0.25, 2.5, 25 and 100 mg L⁻¹. The numbers of microplastic particles per treatment (mL⁻¹) were estimated using haemocytometer (Green et al., 2017, 2019) as 7, 55, 650, 6000 and 22,000 particles mL⁻¹. The low concentration of 0.025 mg L⁻¹ were environmentally realistic (Green et al., 2017, 2019; Sussarellu et al., 2016; Zhang et al., 2019a) and the high concentrations were set to test the tolerance of *U. prolifera* to MPs and the potential of this plant to bioremediate MPs polluted waters. The cultures were bubbled with filtered air (0.22 μm) in seawater and conducted for seven days. The exposure period was according to the previous studies on MPs for algae (Guo et al., 2020). The old medium was renewed with the new medium with the setting MPs concentration every two days and each treatment was quintuplicated.

The relative growth rate (RGR) was estimated as follows: RGR (%) = (lnM_{t2} - lnM_{t1}) / t × 100, where M_{t1} is the initial fresh mass for adults; M_{t2} is the fresh mass after t days culture. The photosynthetic parameters were measured by a pulse modulation fluorometer (WaterPAM, Walz, Germany). The actinic light was set as 240 μmol photons m⁻² s⁻¹ to be consistent with the culture light intensity and the saturating pulse was 5000 μmol photons m⁻² s⁻¹ (0.8 s). Effective photochemical efficiency of PSII = (Fm' - Ft)/Fm' and nonphotochemical quenching (NPQ) was calculated as follows: NPQ = (Fm - Fm') / Fm', where Fm' is the maximum fluorescence yield under actinic light, Ft is the fluorescence at an excitation level and Fm is the maximum fluorescence yield after 15 min dark adaptation. The rapid light curves for relative electron transport rate (rETR) were measured under 11 different PAR levels with every measurement lasting 10 s. The parameters of electron transport efficiency (α), maximum rETR (rETR_{max}) and saturating irradiance (I_k) were calculated from the rETR curves (Fig. S2) following the model (Eilers and Peeters, 1988): rETR = I / (a × I² + b × I + c), α = 1 / c, rETR_{max} = 1 / [b + 2 × (a × c)^{1/2}], I_k = rETR_{max} / α, where I is the incident irradiance; a, b, and c are the adjustment parameters.

2.7. Data analysis

The data were analyzed using the software SPSS v.23. The data under every treatment conformed to a normal distribution (Shapiro-Wilk, *P* > 0.05) and the variances could be considered homogeneous (Levene's test, *P* > 0.05). Two-way analysis of variance (ANOVA) was conducted to assess the effect of area and ecological niche (drifting and attached) on the abundance of MPs and meso- & macroplastics in thalli and seawater, and the ratio of plastics abundance in thalli to that in seawater (Table S2). Curve fitting was conducted to analyze the relationship between size distribution and abundance of plastics in each area. One-way ANOVA was conducted to assess difference of MPs proportion among shapes, colours or material types in each location, and the effect of MPs on physiological parameters of *U. prolifera*. Fisher Least significant difference (Fisher LSD) was conducted for ANOVA *post hoc* investigation. A confidence interval of 95 % was set for all tests.

3. Results

3.1. Plastics in drifting and attached *U. prolifera*

Our procedural blanks showed only 2.08 ± 1.31 particles/batch, much lower than the average abundance of plastics for samples (661 ± 331.56 particles/batch), indicating the reliability of quality control. Two-way ANOVA analysis showed that *U. prolifera* in different areas had different MPs abundance (*F*_{3, 85} = 3.014, *P* = 0.034, Fig. 2a) and drifting thalli trapped more plastics than attached thalli (*F*_{1, 85} = 4.320, *P* = 0.041, Fig. 2a), while no interactive effects were found between area and ecological niche (*F*_{3, 85} = 1.974, *P* = 0.124). More interesting, in drifting thalli, the abundance of MPs increased with the increase of its migration distance, with the highest abundance (1.48 ± 1.39 particles/g) found in QD and the lowest abundance

(0.42 ± 0.23 particles/g) in YC; while this trend was not found in attached *U. prolifera*. For meso- and macroplastics, only areas affected their abundance in *U. prolifera* (*F*_{3, 85} = 3.289, *P* = 0.025, Fig. 2b) while the difference between drifting and attached thalli was not statistically significant (*F*_{1, 85} = 1.879, *P* = 0.174, Fig. 2b). The abundance of meso- and macroplastics in drifting *U. prolifera* decreased with the increase of its migration distance, with the highest abundance in YC (0.28 ± 0.16 particles/g) and the lowest in QD (0.02 ± 0.02 particles/g).

The MPs abundance in nearshore seawater was commonly higher than that in offshore seawater although the differences were not statistically significant (*F*_{1, 23} = 3.590, *P* = 0.071, Fig. 2c). There was a significant difference between areas from south to north (*F*_{3, 23} = 4.795, *P* = 0.010); the highest abundance was found in nearshore seawater in LYG (1.59 ± 0.84 particles/L) and lowest was in offshore seawater in RZ (0.07 ± 0.06 particles/L). For meso- and macroplastics (Fig. 2d), the pattern was similar; there were no significant differences between offshore and nearshore seawaters (*F*_{1, 23} = 1.374, *P* = 0.258) but the difference between areas from south to north was significant (*F*_{3, 23} = 6.112, *P* = 0.003). The highest abundance was also found in LYG for both offshore and nearshore seawaters.

To assess the capacity of *U. prolifera* trapping plastics, the ratios of plastics abundance in *U. prolifera* to that in seawater were calculated (Fig. 2e, f). Two-way ANOVA analysis showed that the ratios for MPs changed in different areas (*F*_{3, 85} = 5.264, *P* = 0.002, Fig. 2e) and drifting thalli usually had higher ratios than attached thalli (*F*_{1, 85} = 10.122, *P* = 0.002, Fig. 2e). The highest ratio (3916.84 ± 4038.72) occurred in drifting thalli in QD. In terms of meso- and macroplastics, drifting thalli had higher values than attached thalli (*F*_{1, 85} = 8.459, *P* = 0.005, Fig. 2f) whereas the differences among areas were not statistically significant (*F*_{3, 85} = 1.079, *P* = 0.362, Fig. 2f).

To explore the reasons why *U. prolifera* has such strong capacity to trap MPs, the trapping mechanisms of MPs in the samples from each sampling station was examined. Four forms of thalli trapping MPs were found and they can be defined as twining, attachment, embedment and wrapping (Fig. 3a-f). Attachment (48 %) and twining (37 %) were the dominant trapping mechanisms, with wrapping and embedment accounting for 11 % and 4%, respectively. Different shapes of plastics were found wrapped in thallus air sacs, including microbead, foam and film. In contrast with MPs, all meso- & macroplastics were twined with thalli of *U. prolifera* (Fig. 3g-i).

3.2. Size, shape, colour and polymer composition of plastics

In terms of MPs size, it ranged from 13.5 to 4991.1 μm. The abundance of MPs exponentially decreased with the increase of size for both drifting and attached thalli in each area except for the drifting thalli in YC (Fig. 4a-d); the size from 13.5 to 1000 μm accounted for 38.2–72.3 % of the total MPs and the size from 4000 to 4991.1 μm only 0.0 %–8.8 %. In terms of meso- & macroplastics (Fig. 4e-h), the percentage of them also exponentially decreased with the increase of size for drifting thalli except for YC, whereas this pattern only occurred in LYG for attached thalli.

Five shapes of MPs were observed in the samples, including microbead, film, fragment, foam and fiber (Fig. 5a, b). ANOVA analyses showed that different shapes were not equally distributed for either drifting or attached samples at each station (*F* > 62.310, *P* < 0.001), and fiber was the most abundant shape for each area (78.8–93.8 %, Fisher LSD, *P* < 0.05, Fig. 5a, b). Following fiber, foam is the second abundant shape for most areas (Fisher LSD, *P* < 0.05). The colour of MPs was classified to five categories (Fig. 5c, d). White-transparent and black-grey were the dominating colours for both drifting and attached samples except for the attached sample from YC where black-grey and blue-green are the dominating colour. In addition to shape and colour, MPs in the samples were identified as nine main types, including polyethylene (PE), polystyrene (PS), polypropylene (PP), polyamide

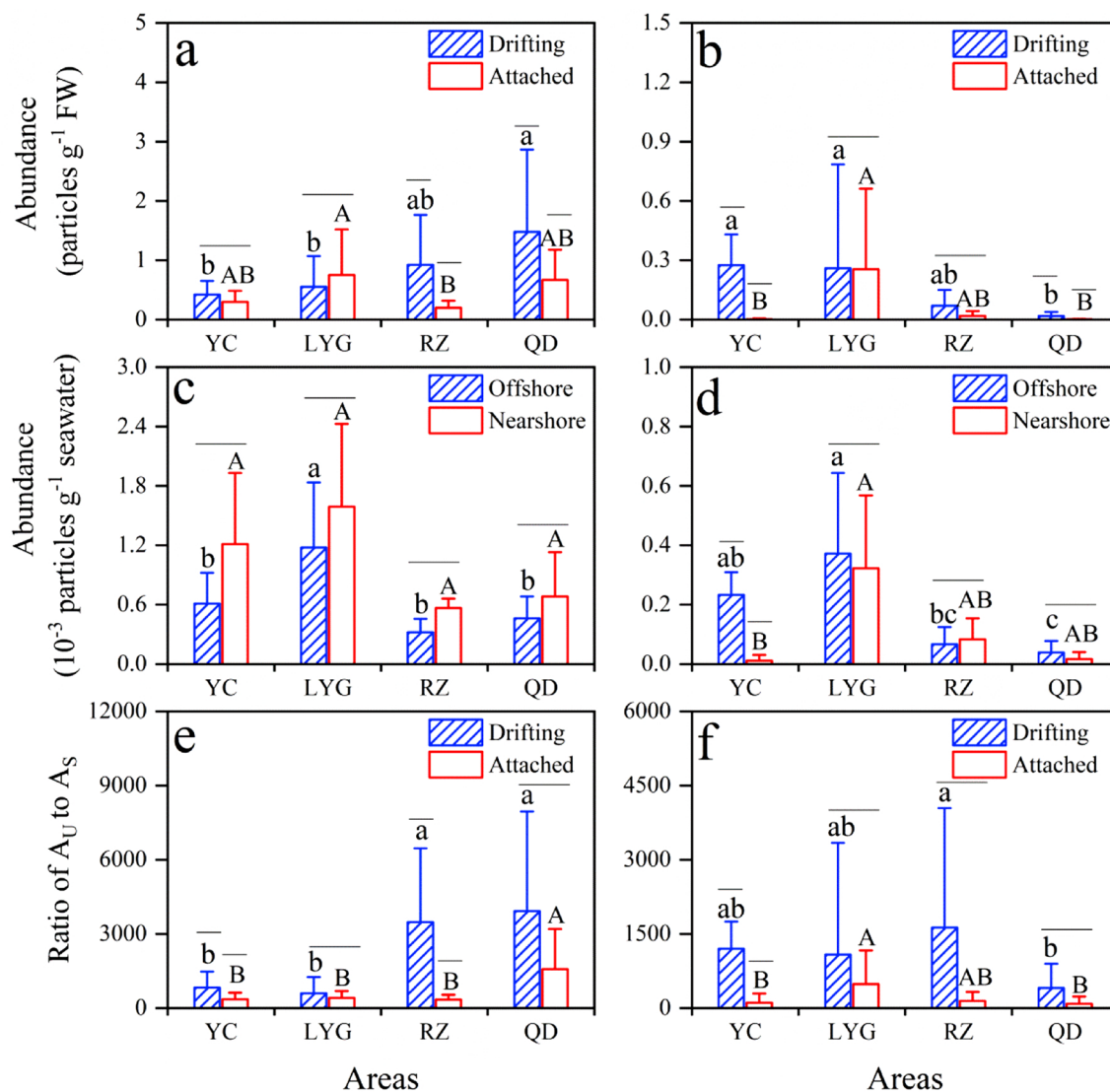


Fig. 2. Abundance of microplastics (a, c) and meso- & macroplastics (b, d) in drifting and attached *U. prolifera* (a, b) or in seawater (c, d), and the ratio of abundance of microplastics (e) and meso- & macroplastics (f) in *U. prolifera* (A_U) to that in seawater (A_S) in different areas. YC, Yancheng; LYG, Lianyungang; RZ, Rizhao; QD, Qingdao. In each panel, horizontal short lines represent the significant difference between drifting and attached samples for each area; different small and block letters represent the significant difference (Fisher LSD, $P < 0.05$) among areas for drifting and attached samples, respectively. The data are presented as mean values and the error bars indicate the standard deviations.

(PA), polyethylene terephthalate (PET), rayon, poly (ethylene: propylene) (PE-PP), polyvinyl chloride (PVC) and polyether polyurethane (PEU), with those accounting for $< 1\%$ (polyester, polyacrylonitrile, cellophane, poly tetra fluoro ethylene, alkyd resin, poly methyl methacrylate, poly (ethylene: vinyl alcohol), polycarbonate, polyacrylamide, poly (styrene: acrylate), phenol formaldehyde resin, poly (acrylonitrile: butadiene: styrene)) being defined as others (Fig. 5e, f). Polyethylene (PE) was the dominating material type for both drifting and attached samples in each area except LYG where PS had the highest proportion in the attached *U. prolifera*.

Compared to MPs, meso- and macroplastics had less diversity in shape, colour and material type (Fig. 6). Fiber was the only shape for all attached *U. prolifera* and drifting *U. prolifera* in RZ, accounting for about 90 % for drifting thalli in other areas (Fig. 6a, b). In terms of colour, there were more colour forms in drifting samples compared to attached samples that had only black-gray in YC and QD, white-transparent, black-gray and blue-green in LYG (Fig. 6c, d). The similar pattern was found in material type; there were at least three material types found in

the drifting thalli for each area while only rayon were found in QD and only PE and PP were found in YC and RZ for the attached thalli (Fig. 6e, f). The spectra of the nine dominant material types matched more than 75 % that of the standard materials (Fig. S3).

3.3. Effects of MPs on *U. Prolifera*

ANOVA analysis and *Post hoc* Fisher LSD comparison showed that MPs did not affect relative growth rate of *U. prolifera* until it reached the extremely high concentration (100 mg L^{-1}) ($F_{5, 24} = 6.141$, $P = 0.001$, Fig. 7a). The same trend was found in effective photochemical efficiency of PSII (Fig. 7b). The higher MPs levels ($2.5\text{--}25 \text{ mg L}^{-1}$) enhanced NPQ and then reduced it at highest MPs level ($F_{5, 24} = 68.369$, $P < 0.001$, Fig. 7c). MPs did not affect rETR_{max} until it reached the highest level ($F_{5, 24} = 2.845$, $P = 0.037$, Fig. 7d). Meanwhile, the highest MPs level also reduced α ($F_{5, 24} = 23.109$, $P < 0.001$, Fig. 7e) but increased I_k ($F_{5, 24} = 28.824$, $P < 0.001$, Fig. 7f).

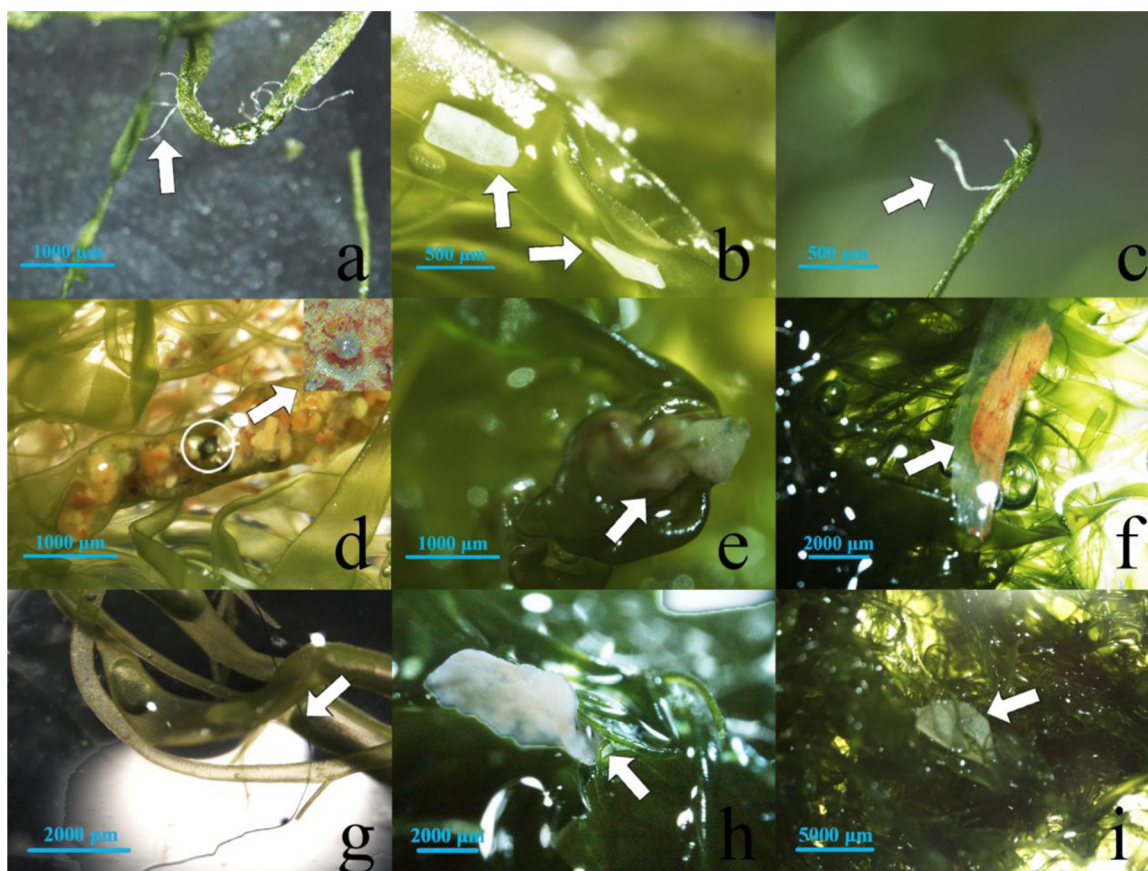


Fig. 3. Mechanisms of *U. prolifera* trapping microplastics (a-f) and meso- & macroplastics (g-i). (a, g, h, i) twining, (b) attachment, (c) embedment, and (d, e, f) wrapping. Different plastic were wrapped in the tubular air sac of *U. prolifera*, including microbead (d), foam (e) and film (f).

4. Discussion

4.1. Trapping capacity of *U. prolifera* for MPs

The average abundance of MPs in drifting *U. prolifera* was 0.83 ± 0.95 particles/g fresh weight, which is much higher than the levels in seawater and sediments of the Yellow Sea, and also higher than that in zooplankton, oyster and most fish in Yellow Sea and East China Sea (Table 1). The average ratio of MPs abundance in *U. prolifera* to that in seawater was more than 2000. This strong trapping capacity may result from the whole-thallus trapping and fast growth of *U. prolifera*. MPs can exist in the whole thallus of *U. prolifera* while usually in digestive tissues for marine animals (Duncan et al., 2019; Law, 2017; Wang et al., 2019b,2019a). In addition, at least four mechanisms for *U. prolifera* to trap plastics were found in the present study, which also contribute to its strong trapping capacity of MPs. It has been reported recently that MPs could adhere to the surface of the red macroalgae *Pyropia* spp. and the seagrasses *Zostera marina* and *Thalassia testudinum* (Goss et al., 2018; Jones et al., 2020; Li et al., 2020). This study demonstrates that MPs can be twined, embedded and even wrapped in the air sac of *U. prolifera* apart from adherence to the surface of thalli, which contributes to its higher trapping capacity compared to *Pyropia* spp. (Table 1). The diverse MPs trapping mechanisms of *U. prolifera* could be attributed to its unique morphology that features a hollow tubular body composed of monolayer cells and highly branches under some environments (Gao et al., 2016). In addition, the cell wall of *U. prolifera* is mainly composed of sulfated polysaccharide that may play an important role in adsorbing MPs (Chi et al., 2018). The annual biomass of *Ulva* green tides has been shown to range 6–65 million tons in the Yellow Sea of China during past ten years (State Oceanic Administration SOA, 2018), which can trap as much as 4.98–53.95

trillion (10^{12}) particles of MPs based on the present study.

4.2. Characteristics of MPs trap in *U. prolifera* during migration

It is worth noting that the richer abundance of MPs in drifting *U. prolifera* coincided well with its longer migration distance, while more meso- and macroplastics were observed with shorter migration path of the alga. Considering that these patterns were not found in attached *U. prolifera*, they may be related to the plastic trap and detachment during the long-distance migration. Among the four trapping mechanisms, twining and attachment are the major mechanisms that *U. prolifera* traps plastics and it seems that twining and attached plastics are easier to be detached from the thalli compared to embedded and wrapping ones, making plastics trapping in *U. prolifera* change with the migration path. Different from four mechanisms found for MPs, all meso- and macroplastics were twined by thalli of *U. prolifera*, which may make them easier to be detached by wind and wave and result in the decrease of meso- and macroplastics abundance and increase of MPs abundance in *U. prolifera* with the migration of green tides from south to north of the Yellow Sea. In addition, these patterns may also be due to the degradation of meso- and macroplastics into MPs by mechanical abrasion and photodegradation during the migration (Barnes et al., 2009; Khoironi et al., 2020). Compared to larger MPs, smaller MPs with same mass can carry more toxic matters and are more difficult to remove as well (Betts, 2008; Wang et al., 2019b,2019a). *Ulva* species can be consumed by benthic, pelagic and nektonic herbivore (Diop et al., 2016; Long et al., 2011) and furthermore it can also be incorporated in terrestrial food web (Catenazzi and Donnelly, 2007). Therefore, more MPs with smaller size in *U. prolifera* at the ending sites of green tides suggests larger potential risk not only for itself and but also for other organisms through food chain.

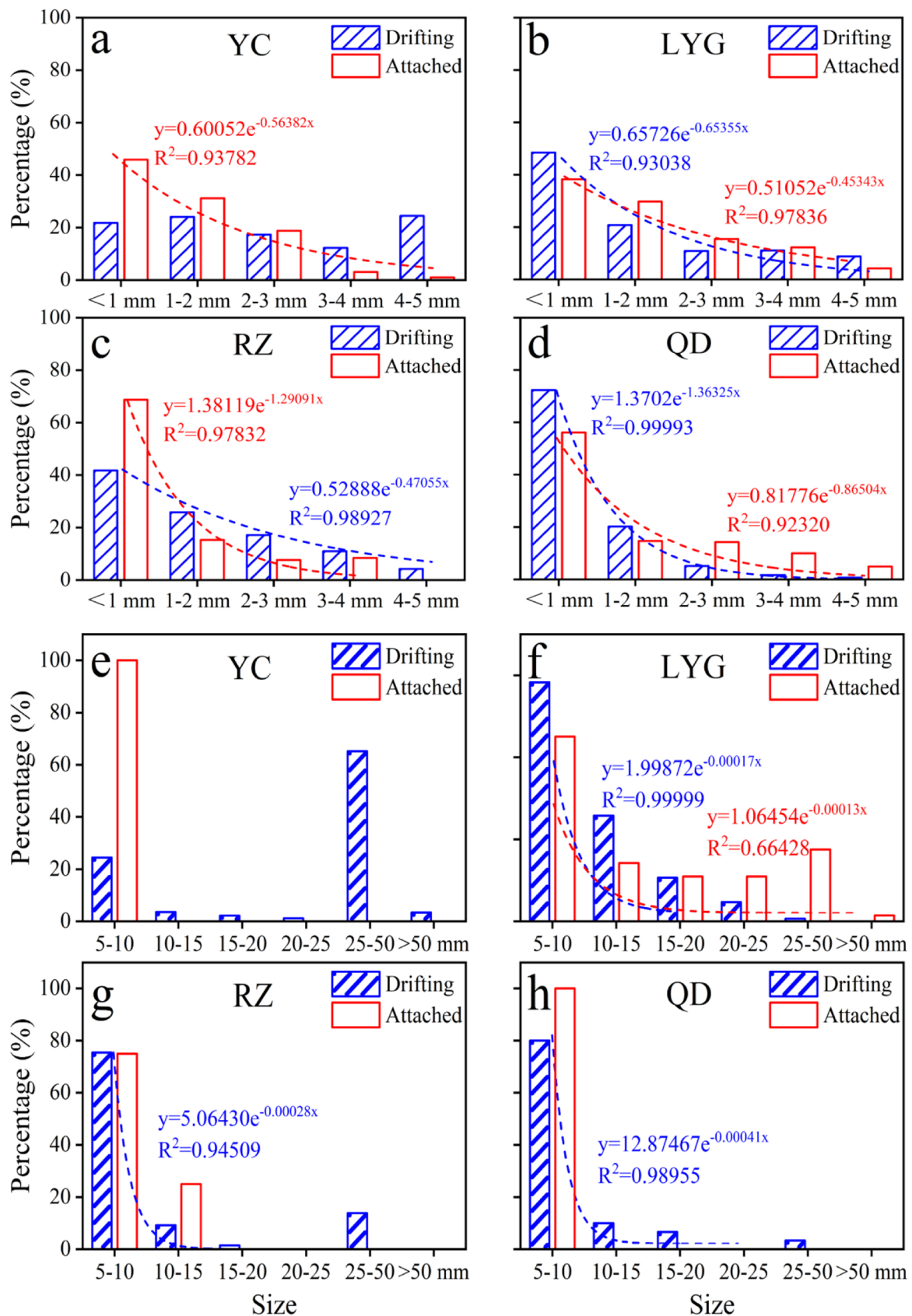


Fig. 4. Size distribution of MPs (a-d) and meso- & macroplastics (e-h) in drifting and attached *U. prolifera* in different areas. YC, Yancheng; LYG, Lianyungang; RZ, Rizhao; QD, Qingdao.

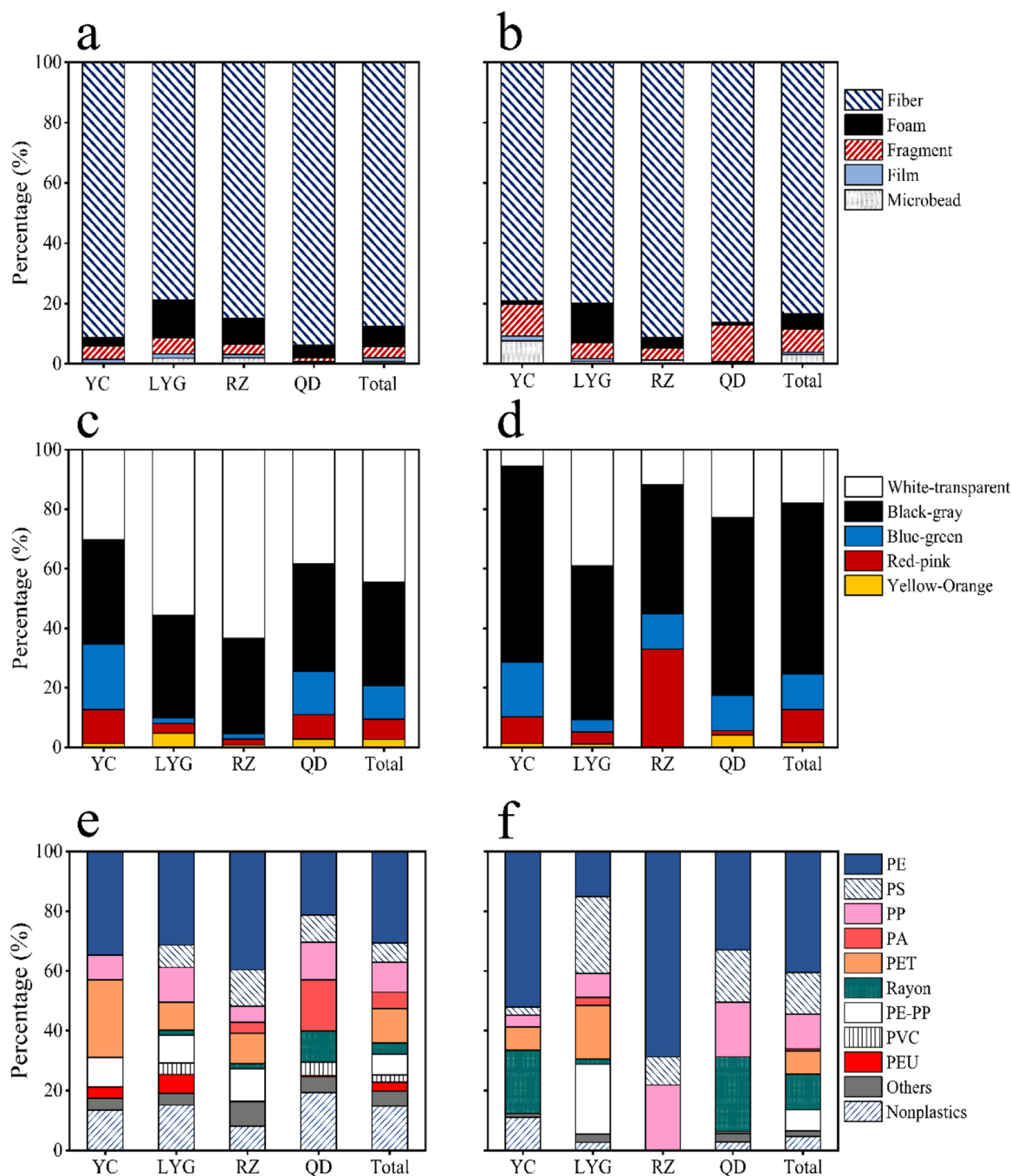


Fig. 5. The shape (a, b), colour (c, d) and material type (e, f) of microplastics in drifting (a, c, e) and attached (b, d, f) *U. prolifera* in each area. YC, Yancheng; LYG, Lianyungang; RZ, Rizhao; QD, Qingdao.

Among the MPs detected, fiber was the most common shape in *U. prolifera*. This is consistent with previous studies on MPs in zooplankton, shellfish and fish in the Yellow Sea (Feng et al., 2019; Qu et al., 2018; Sun et al., 2018). The microplastic polymer type was dominated by PE, which is similar to the case in seawater and sediment in the Yellow Sea (Sun et al., 2018; Zhao et al., 2018). The dominant PE and fibers in *U. prolifera* should originate from aquaculture industry that is flourishing in the Yellow Sea. PE fiber is commonly used as ropes and fishing nets for seaweed cultivation and marine animal aquaculture (Andrady, 2011; Remy et al., 2015). The degradation of these ropes and fishing nets can generate a large number of MPs (Cheng et al., 2018; Feng et al., 2020). Meanwhile, PE is considered as synthetic fibers from clothes and thereby PE fiber can come from domestic wastewater as well (Wang et al., 2019c).

Colour can affect MPs ingestion by organisms and it has been reported that animals prefer to ingest MPs with similar colour to their prey (Ory et al., 2017; Xiong et al., 2019). Meanwhile, Santos et al. (2016) demonstrated that the influence of colour on MP ingestion follows Thayer's law "marine animals that perceive drifting plastic from below should preferentially ingest dark plastic fragments, whereas animals that perceive drifting plastic from above should select for paler plastic fragments." In the present study, drifting thalli trapped more white-transparent plastics while attached thalli trapped more black-gray plastics. Based on the conclusions from the studies mentioned above, MPs on *U. prolifera* would ease thalli consumption by herbivores for both drifting and attached ecological niches.

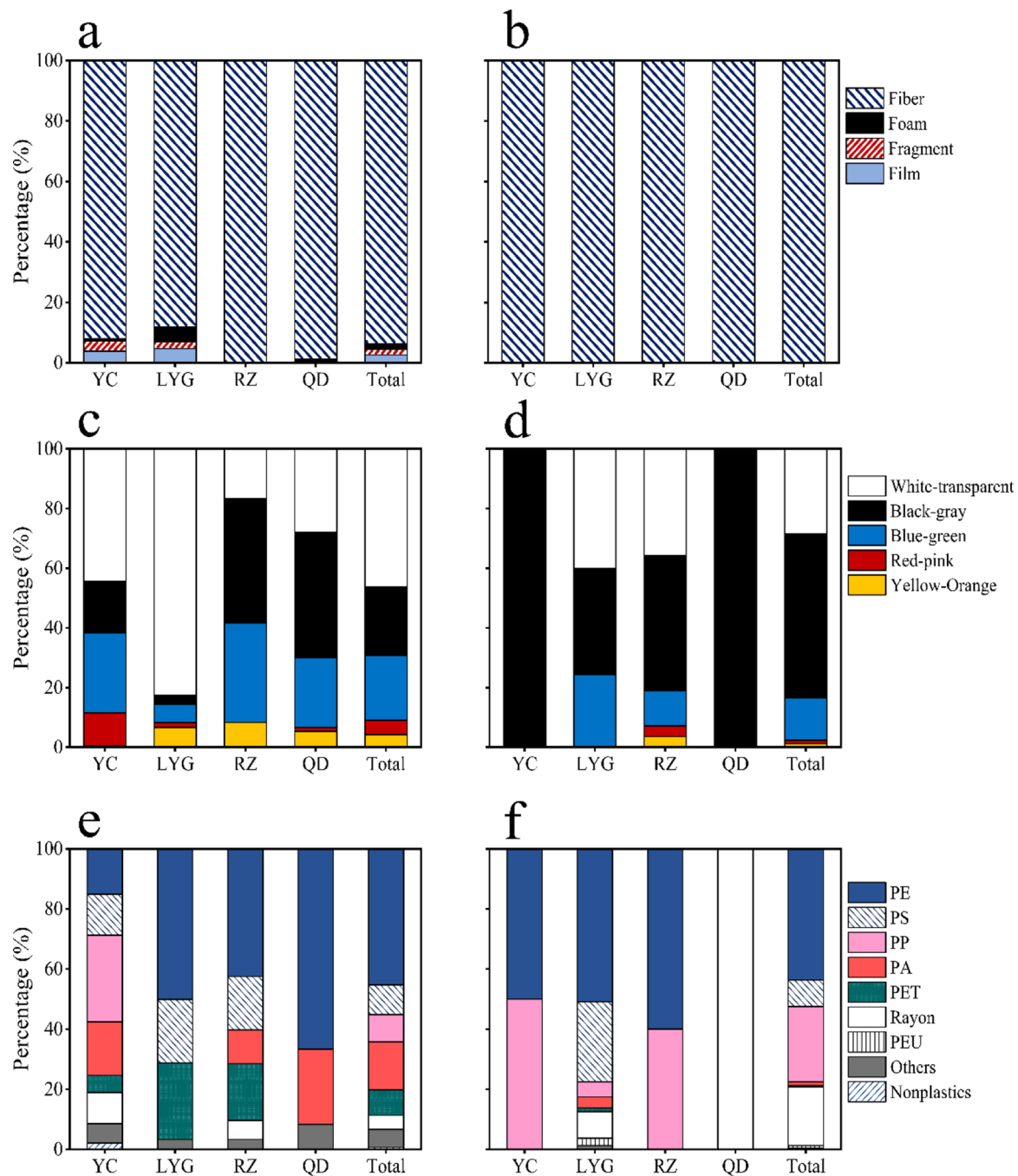


Fig. 6. The shape (a, b), colour (c, d) and material type (e, f) of meso- & macroplastics in drifting (a, c, e) and attached (b, d, f) *U. prolifera* in each area. YC, Yancheng; LYG, Lianyungang; RZ, Rizhao; QD, Qingdao.

4.3. Impact of MPs in macroalgae

The drifting *U. prolifera* plants maintain the MPs in the surface seawater during the development of green tides; however, when the tides start to degrade in later phase, tubular air sac in *U. prolifera*'s thalli will be ruptured, resulting in sinking of the algal biomass (Zhang et al., 2013a, b). The associated MPs may sink with *Ulva* thalli together to sediment or released to seawater. On the other hand, some meso- and macroplastics in the bottom layer of water column or sea floor in the intertidal zone may be transported upward when naturally attached *U. prolifera* became drifting due to tide forcing and/or biotic disturbances. Therefore, the drifting macroalgae can affect the distribution of plastics both spatially and temporally via their trap and release. Macroalgae usually live in the littoral zones. However, increasingly drifting forms of

macroalgae dramatically expands their distribution areas and thus the risk of MPs transport and transmission. Gutow et al. (2015) has showed that benthic marine meso-herbivores can ingest MPs by consuming MPs-contaminated seaweeds. Our study suggests that drifting seaweeds can also trap MPs that could be transmitted to higher trophic levels if drifting seaweeds are consumed by planktonic herbivores, such as rabbitfish *Siganus canaliculatus* (You et al., 2014a, 2014b). In comparison with red tides, green tides have been considered as harmless or less harmful to other organisms because they do not produce toxins (Smetacek and Zingone, 2013). However, our findings suggest that green tides could be harmful due to the large amount of MPs that they carry. More importantly, *Ulva* species are used as food in Asian countries and condiments in European countries (Gao et al., 2018b; Peñá-Rodríguez et al., 2011), and therefore MPs in *Ulva* can be transferred to

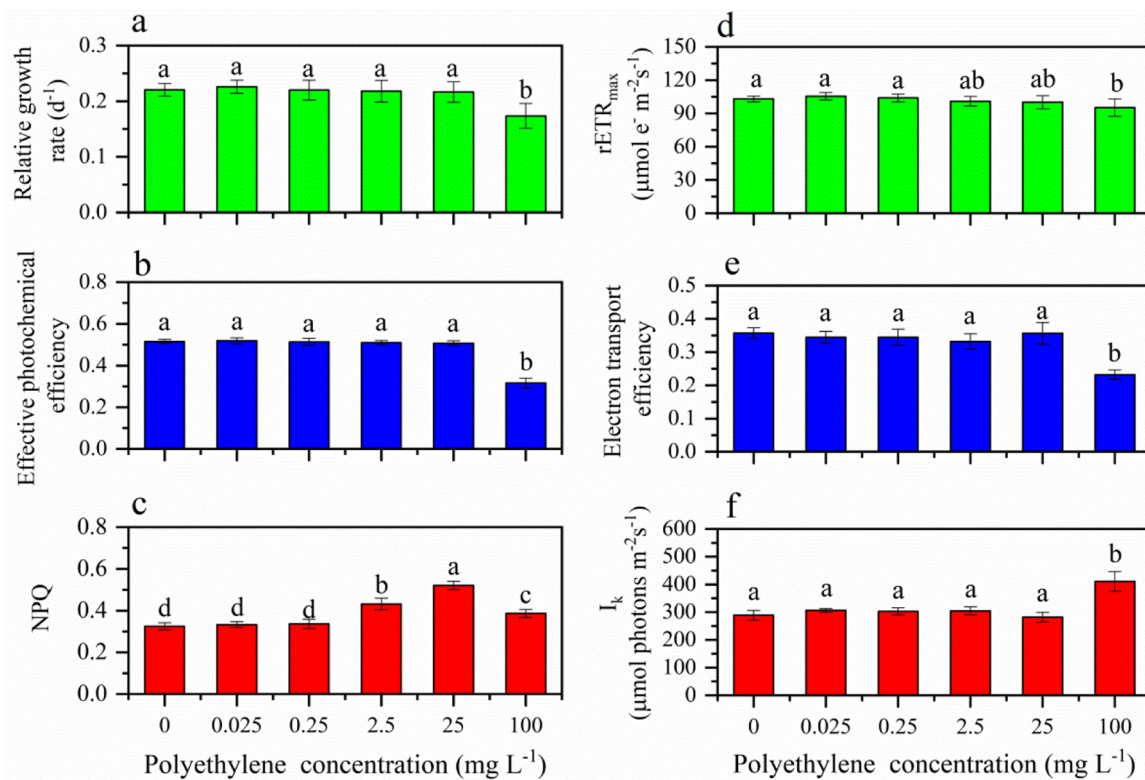


Fig. 7. Effects of polyethylene particle on relative growth rate (a), effective photochemical efficiency (b), nonphotochemical quenching (NPQ, c), maximum rETR ($rETR_{max}$, d), electron transport efficiency (α , e), and saturating irradiance (I_k , f) of *U. prolifera*. The error bars indicate the standard deviations ($n = 5$). Different letters represent the significant difference (Fisher LSD, $P < 0.05$) among polyethylene particle concentrations.

mankind and directly threaten human health as shown in nori (Li et al., 2020).

4.4. Using macroalgae to deal with MPs pollution in marine environment

The MPs of polyethylene do not affect growth or photosynthetic performance of *U. prolifera* until it reaches a very high concentration. This indicates that *U. prolifera* has a high tolerance to MPs, which contributes to the explanation of the robustness of this species in the field. The negligible effect of MPs on *U. prolifera* indicates that this species may be a potential bio-trapper for MPs. On the other hand, the highest concentration of polyethylene significantly reduced the growth rate of *U. prolifera*. This can be related to the decreased effective

photochemical efficiency of PSII as inhibited effective photochemical efficiency of PSII and photosynthesis usually result in reduced growth rate (Gao et al., 2017b; Yue et al., 2019). Furthermore, the highest concentration of polyethylene reduced α , $rETR_{max}$ but enhanced saturating irradiance, indicating that the negative effect of MPs on photosynthetic performance could be due to the shading effect after they attaches to the surface of thalli (Fig. S4). It is worth noting that the lower MPs levels (2.5–25 mg L⁻¹) induced higher NPQ although growth or effective photochemical efficiency was not affected. NPQ is a signal that cells are experiencing and responding to environmental stress (Gao et al., 2017b; Kitao et al., 2019). Cells activated more NPQ to deal with the stress of MPs at the lower MPs levels while the highest MPs level inhibited the capacity of NPQ and thus led to the decrease of

Table 1
Microplastics abundance in seawater and organisms in the seas of China.

Area	Type of mediums	Total species	MPs abundance (particles/g)	References
East China Sea	Bethopelagic fish	4	0.02–0.06	Jabeen et al. (2017) ^a
East China Sea	Demersal fish	11	0.02–0.25	Jabeen et al. (2017) ^a
Yellow Sea	Seaweed	/	0.11–0.31 ^b	(Li et al., 2020)
Yellow Sea	Filter-feeding fish	1	2.41	Feng et al. (2019) ^a
Yellow Sea	Predatory fish	5	0.16–0.39	Feng et al. (2019) ^a
Yellow Sea	Oysters	4	0.25–0.77	Teng et al. (2019)
Yellow Sea	Zooplankton	11	$(12.24 \pm 25.70) \times 10^{-6}$	Sun et al. (2018)
Yellow Sea	Seawater (trawling sample)	/	$(0.13 \pm 0.20) \times 10^{-6}$	Sun et al. (2018)
Yellow Sea	Sediments	/	$(0.037 \pm 0.043) \times 10^{-6}$	Zhu et al. (2018)
Yellow Sea	Seawater (direct sample) ^c	/	$(545 \pm 282) \times 10^{-6}$	Zhu et al. (2018)
Yellow Sea	Seawater (direct sample) ^c	/	$(818 \pm 592) \times 10^{-6}$	This study
Yellow Sea	Drifting <i>U. prolifera</i>	1	0.83 ± 0.95	This study
Yellow Sea	Attached <i>U. prolifera</i>	1	0.49 ± 0.53	This study

^a The data were recalculated based on the fresh weight of the whole individual.

^b The data were obtained based on the mean psychrometric ratio of 9.03 %.

^c Direct sample refers to collecting seawater by water sampler directly and filtering through steel sieve.

effective photochemical efficiency and growth. A similar trend was also found in *U. prolifera* in respond to the combination of ocean acidification and copper (Gao et al., 2017b). In summary, our study suggests that macroalgae seem to have a high tolerance to MPs, which enable it a solid intermediate to transmit MPs to higher trophic levels and an ideal material to treatment MPs in seawaters.

Although MPs pollution in the oceans is becoming a serious challenge to marine environment (Howard, 2018), little is known how to deal with this problem except reducing discharge from the lands. Huang et al. (2019) showed that Seagrass beds could act as a trap of MPs in the nearshore. This study shows that drifting macroalgae can effectively trap MPs in the oceans. Collecting drifting macroalgae can be a way to reduce MPs abundance in seawaters. The drifting *U. prolifera* that originate from Subei shoal in Jiangsu province are eventually landed along the coast of Qingdao in Shandong province annually due to the ocean currents (Liu et al., 2013; Song et al., 2015). Therefore, it is easy to reduce the MPs pollution via collecting the macroalgae along the coast.

5. Conclusions

This study investigated the *in situ* status of plastics in bloom-forming macroalgae for the first time. Taking the world's largest green tide as an example, we found that both drifting and attached *Ulva* species could trap a large amount of plastics via diverse mechanisms. The drifting macroalgae can affect the spatiotemporal distribution of plastics in oceans. The strong trapping capacity of MPs and high tolerance to MPs indicate *Ulva* species a potential material to remediate MPs-polluted seawaters. With the rise of marine plastics as well as macroalgal bloom, the interaction of marine plastics and algal bloom needs more attention.

CRediT authorship contribution statement

Zhihua Feng: Conceptualization, Methodology, Formal analysis, Visualization, Writing - review & editing, Supervision, Funding acquisition. **Tao Zhang:** Conceptualization, Methodology, Visualization, Writing - review & editing. **Huahong Shi:** Writing - review & editing. **Kunshan Gao:** Writing - review & editing. **Wei Huang:** Methodology. **Juntian Xu:** Funding acquisition. **Jiaxuan Wang:** Investigation, Formal analysis, Visualization. **Rui Wang:** Investigation. **Ji Li:** Writing - review & editing. **Guang Gao:** Conceptualization, Methodology, Formal analysis, Visualization, Writing - original draft, Writing - review & editing, Supervision.

Declaration of Competing Interest

The authors declare that they have no known competing financial interests or personal relationships that could have appeared to influence the work reported in this paper.

Acknowledgments

This work was supported by the National Key Research and Development Program of China (2018YFD0900703), the Open-end Funds of Jiangsu Key Laboratory of Marine Bioresources and Environment (SH20191205), the Science Foundation of Huaihai Institute of Technology (Z2015010, KQ19011), the Lianyungang Innovative and Entrepreneurial Doctor Program (201702), China-APEC Cooperation Fund(2029901), Postgraduate Research & Practice Innovation Program of Jiangsu Province (KYCX19-2286) and the Priority Academic Program Development of Jiangsu Higher Education Institutions.

Appendix A. Supplementary data

Supplementary material related to this article can be found, in the

online version, at doi:<https://doi.org/10.1016/j.jhazmat.2020.122752>.

References

- Andrady, A.L., 2011. Microplastics in the marine environment. *Mar. Pollut. Bull.* 62, 1596–1605.
- Arroyo, N.L., Bonsdorff, E., 2016. The role of drifting algae for marine biodiversity. In: Ólafsson, E. (Ed.), *Marine Macrophytes as Foundation Species*. CRC Press, Florida, pp. 285.
- Auta, H.S., Emenike, C.U., Fauziah, S.H., 2017. Distribution and importance of microplastics in the marine environment: a review of the sources, fate, effects, and potential solutions. *Environ. Int.* 102, 165–176.
- Barnes, D.K.A., Galgani, F., Thompson, R.C., Barlaz, M., 2009. Accumulation and fragmentation of plastic debris in global environments. *Philos. Trans. Biol. Sci.* 364, 1985–1998.
- Betts, K., 2008. Why small plastic particles may pose a big problem in the oceans. *Environ. Sci. Technol.* 42, 8995.
- Cai, H., Du, F., Li, L., 2019. A practical approach based on FT-IR spectroscopy for identification of semi-synthetic and natural celluloses in microplastic investigation. *Sci. Total Environ.* 669, 692–701.
- Catenazzi, A., Donnelly, M.A., 2007. The *Ulva* connection: marine algae subsidize terrestrial predators in coastal Peru. *Oikos* 116, 75–86.
- Cheng, Z., Li, H., Yu, L., Yang, Z., Xu, X., Wang, H., Wang, M., 2018. Phthalate esters distribution in coastal mariculture of Hong Kong, China. *Environ. Sci. Pollut. R.* 25, 17321–17329.
- Chi, Y., Li, Y., Zhang, G., Gao, Y., Ye, H., Gao, J., Wang, P., 2018. Effect of extraction techniques on properties of polysaccharides from *Enteromorpha prolifera* and their applicability in iron chelation. *Carbohydr. Polym.* 181, 616–623.
- Diop, M., Howsam, M., Diop, C., Goossens, J.F., Diouf, A., Amara, R., 2016. Assessment of trace element contamination and bioaccumulation in algae (*Ulva lactuca*), mussels (*Perna perna*), shrimp (*Penaeus kerathurus*), and fish (*Mugil cephalus*, *Saratherondon melanotheron*) along the Senegalese coast. *Mar. Pollut. Bull.* 103, 339–343.
- Duncan, E.M., Broderick, A.C., Fuller, W.J., Galloway, T.S., Godfrey, M.H., Hamann, M., Limpus, C.J., Lindeque, P.K., Mayes, A.G., Omeyer, L.C.M., Santillo, D., Snape, R.T.E., Godley, B.J., 2019. Microplastic ingestion ubiquitous in marine turtles. *GCB Bioenergy* 25, 744–752.
- Eilers, P.H.C., Peeters, J.C.H., 1988. A model for the relationship between light intensity and the rate of photosynthesis in phytoplankton. *Ecol. Model.* 42, 199–215.
- Enfrin, M., Dumée, L.F., Lee, J., 2019. Nano/microplastics in water and wastewater treatment processes-Origin, impact and potential solutions. *Water Res.* 161, 621–638.
- Feng, Z., Zhang, T., Li, Y., He, X., Wang, R., Xu, J., Gao, G., 2019. The accumulation of microplastics in fish from an important fish farm and mariculture area, Haizhou Bay, China. *Sci. Total Environ.* 696, 133948.
- Feng, Z., Zhang, T., Wang, J., Huang, W., Wang, R., Xu, J., Fu, G., Gao, G., 2020. Spatio-temporal features of microplastics pollution in macroalgae growing in an important mariculture area, China. *Sci. Total Environ.* 719, 137490.
- Fenton, H.J.H., 1894. Oxidation of tartaric acid in presence of iron. *J. Chem. Soc.* 65, 899–910.
- Galloway, T.S., Cole, M., Lewis, C., 2017. Interactions of microplastic debris throughout the marine ecosystem. *Nat. Ecol. Evol.* 1, 0116.
- Gao, S., Chen, X., Yi, Q., Wang, G., Pan, G., Lin, A., Peng, G., 2010. A strategy for the proliferation of *Ulva prolifera*, main causative species of green tides, with formation of sporangia by fragmentation. *PLoS One* 5, e8571.
- Gao, G., Zhong, Z., Zhou, X., Xu, J., 2016. Changes in morphological plasticity of *Ulva prolifera* under different environmental conditions: a laboratory experiment. *Harmful Algae* 59, 51–58.
- Gao, G., Clare, A.S., Rose, C., Caldwell, G.S., 2017a. Eutrophication and warming-driven green tides (*Ulva rigida*) are predicted to increase under future climate change scenarios. *Mar. Pollut. Bull.* 114, 439–447.
- Gao, G., Liu, Y., Li, X., Feng, Z., Xu, Z., Wu, H., Xu, J., 2017b. Expected CO₂-induced ocean acidification modulates copper toxicity in the green tide alga *Ulva prolifera*. *Environ. Exp. Bot.* 135, 63–72.
- Gao, G., Beardall, J., Bao, M., Wang, C., Ren, W., Xu, J., 2018a. Ocean acidification and nutrient limitation synergistically reduce growth and photosynthetic performances of a green tide alga *Ulva linza*. *Biogeosciences* 15, 3409–3420.
- Gao, G., Clare, A.S., Chatzidimitriou, E., Rose, C., Caldwell, G., 2018b. Effects of ocean warming and acidification, combined with nutrient enrichment, on chemical composition and functional properties of *Ulva rigida*. *Food Chem.* 258, 71–78.
- Gao, G., Clare, A.S., Rose, C., Caldwell, G.S., 2018c. *Ulva rigida* in the future ocean: potential for carbon capture, bioremediation and biomethane production. *GCB Bioenergy* 10, 39–51.
- Gasper, J., Wright, S.L., Dris, R., Collard, F., Mandin, C., Guerrouache, M., Langlois, V., Kelly, F.J., Tassin, B., 2018. Microplastics in air: are we breathing it in? *Curr. Opin. Environ. Sci. Health* 1, 1–5.
- Goss, H., Jaskiel, J., Rotjan, R., 2018. *Thalassia testudinum* as a potential vector for incorporating microplastics into benthic marine food webs. *Mar. Pollut. Bull.* 135, 1085–1089.
- Green, D.S., Boots, B., O'Connor, N.E., Thompson, R., 2017. Microplastics affect the ecological functioning of an important biogenic habitat. *Environ. Sci. Technol.* 51, 68–77.
- Green, D.S., Colgan, T.J., Thompson, R.C., Carolan, J.C., 2019. Exposure to microplastics reduces attachment strength and alters the haemolymph proteome of blue mussels (*Mytilus edulis*). *Environ. Pollut.* 246, 423–434.
- Guo, Y., Ma, W., Li, J., Liu, W., Qi, P., Ye, Y., Guo, B., Zhang, J., Qu, C., 2020. Effects of microplastics on growth, phenanthrene stress, and lipid accumulation in a diatom,

- Phaeodactylum tricornutum*. Environ. Pollut. 257, 113628.
- Gutow, L., Eckerlebe, A., Giménez, L., Saborowski, R., 2015. Experimental evaluation of seaweeds as a vector for microplastics into marine food webs. Environ. Sci. Technol. 50, 915–923.
- Haward, M., 2018. Plastic pollution of the world's seas and oceans as a contemporary challenge in ocean governance. Nat. Commun. 9, 667.
- He, P., Xu, S., Zhang, H., Wen, S., Dai, Y., Lin, S., Charles, Y., 2008. Bioremediation efficiency in the removal of dissolved inorganic nutrients by the red seaweed, *Porphyra yezoensis*, cultivated in the open sea. Water Res. 42, 1281–1289.
- Hermabessiere, L., Dehaut, A., Paul-Pont, I., Lacroix, C., Jezequel, R., Soufant, P., Duflos, G., 2017. Occurrence and effects of plastic additives on marine environments and organisms: a review. Chemosphere 182, 781–793.
- Huang, Y., Xiao, X., Xu, C., Perianen, Y.D., Hu, J., Holmer, M., 2019. Seagrass beds acting as a trap of microplastics-Emerging hotspot in the coastal region? Environ. Pollut. 257, 113450.
- Hurley, R.R., Lusher, A.L., Marianne, O., Luca, N., 2018. Validation of a method for extracting microplastics from complex, organic-rich, environmental matrices. Environ. Sci. Technol. 52, 7409–7417.
- Isobe, A., Iwasaki, S., Uchida, K., Tokai, T., 2019. Abundance of non-conservative microplastics in the upper ocean from 1957 to 2066. Nat. Commun. 10, 417.
- Jabeen, K., Su, L., Li, J., Yang, D., Tong, C., Mu, J., Shi, H., 2017. Microplastics and mesoplastics in fish from coastal and fresh waters of China. Environ. Pollut. 221, 141–149.
- Jambeck, J.R., Geyer, R., Wilcox, C., Siegler, T.R., Perryman, M., Andrady, A., Narayan, R., Law, K.L., 2015. Plastic waste inputs from land into the ocean. Science 347, 768–771.
- Jones, K.L., Hartl, M.G., Bell, M.C., Capper, A., 2020. Microplastic accumulation in a *Zostera marina* L. Bed at Deerness Sound, Orkney. Scotland. Mar. Pollut. Bull. 152, 110883.
- Khoironi, A., Hadiyanto, H., Anggoro, S., Sudarno, S., 2020. Evaluation of polypropylene plastic degradation and microplastic identification in sediments at Tambak Lorok coastal area, Semarang, Indonesia. Mar. Pollut. Bull. 151, 110868.
- Kitao, M., Tobita, H., Kitaoka, S., Harayama, H., Yazaki, K., Komatsu, M., Agathokleous, E., Koike, T., 2019. Light energy partitioning under various environmental stresses combined with elevated CO₂ in three deciduous broadleaf tree species in Japan. Climate 7, 79.
- Law, K.L., 2017. Plastics in the marine environment. Annu. Rev. Mar. Sci. 9, 205–229.
- Lebreton, L.C.M., Joost, V.D.Z., Damsteeg, J.W., Slat, B., Andrady, A., Reisser, J., 2017. River plastic emissions to the world's oceans. Nat. Commun. 8, 15611.
- Li, Q., Feng, Z., Zhang, T., Ma, C., Shi, H., 2020. Microplastics in the commercial seaweed nori. J. Hazard. Mater. 388, 122060.
- Liu, D., Keesing, J.K., He, P., Wang, D., Shi, Y., Wang, Y., 2013. The world's largest macroalgae bloom in the Yellow Sea, China: formation and implications. Estuar. Coast. Shelf S. 129, 2–10.
- Long, Z.T., Bruno, J.F., Duffy, J.E., 2011. Food chain length and omnivory determine the stability of a marine subtidal food web. J. Anim. Ecol. 80, 586–594.
- Lusher, A.L., Tirelli, V., O'Connor, I., Officer, R., 2015. Microplastics in Arctic polar waters: the first reported values of particles in surface and sub-surface samples. Sci. Rep-UK 5, 14947.
- Murphy, V., Hughes, H., McLoughlin, P., 2007. Cull binding by dried biomass of red, green and brown macroalgae. Water Res. 41, 731–740.
- Oberholster, P.J., Cheng, P.H., Botha, A.M., Genthe, B., 2014. The potential of selected macroalgae species for treatment of AMD at different pH ranges in temperate regions. Water Res. 60, 82–92.
- Ory, N.C., Sobral, P., Ferreira, J.L., Thiel, M., 2017. Amberstripe scad *Decapterus muroadsi* Carangidae fish ingest blue microplastics resembling their copepod prey along the coast of Rapa Nui Easter Island in the South Pacific subtropical gyre. Sci. Total Environ. 586, 430–437.
- Pan, Z., Guo, H., Chen, H., Wang, S., Sun, X., Zou, Q., Zhang, Y., Lin, H., Cai, S., Huang, J., 2019. Microplastics in the Northwestern Pacific: Abundance, distribution, and characteristics. Sci. Total Environ. 650, 1913–1922.
- Peña-Rodríguez, A., Mawhinney, T.P., Ricque-Marie, D., Cruz-Suárez, L.E., 2011. Chemical composition of cultivated seaweed *Ulva clathrata* Roth C. Agardh. Food Chem. 129, 491–498.
- Plastics Europe, 2018. Plastics-the Facts 2017-an Analysis of European Plastics Production, Demand and Waste Data.
- Qu, X., Su, L., Li, H., Liang, M., Shi, H., 2018. Assessing the relationship between the abundance and properties of microplastics in water and in mussels. Sci. Total Environ. 621, 679–686.
- Reed, D., Washburn, L., Rassweiler, A., Miller, R., Bell, T., Harrer, S., 2016. Extreme warming challenges sentinel status of kelp forests as indicators of climate change. Nat. Commun. 7, 13757.
- Remy, F., Collard, F., Gilbert, B., Compère, P., Eppe, G., Lepoint, G., 2015. When microplastic is not plastic: the ingestion of artificial cellulose fibers by macrofauna living in seagrass macrophytodebris. Environ. Sci. Technol. 49, 11158–11166.
- Santos, R.G., Andrades, R., Fardim, L.M., Martins, A.S., 2016. Marine debris ingestion and Thayer's law-The importance of plastic color. Environ. Pollut. 214, 585–588.
- Siripornadulsil, S., Siripornadulsil, W., 2013. Cadmium-tolerant bacteria reduce the uptake of cadmium in rice: potential for microbial bioremediation. Ecotox. Environ. Safe. 94, 94–103.
- Smetacek, V., Zingone, A., 2013. Green and golden seaweed tides on the rise. Nature 504, 84–88.
- Solovchenko, A., Khozin-Goldberg, I., 2013. High-CO₂ tolerance in microalgae: possible mechanisms and implications for biotechnology and bioremediation. Biotechnol. Lett. 35, 1745–1752.
- Song, W., Li, Y., Fang, S., Wang, Z., Xiao, J., Li, R., Fu, M., Zhu, M., Zhang, X., Zhang, X., 2015. Temporal and spatial distributions of green algae micro-propagules in the coastal waters of the Subei Shoal, China. Estuar. Coast. Shelf S. 163, 29–35.
- State Oceanic Administration SOA, 2018. Bulletin of China Marine Disaster 2008.
- Sun, X., Liang, J., Zhu, M., Zhao, Y., Zhang, B., 2018. Microplastics in seawater and zooplankton from the Yellow Sea. Environ. Pollut. 242, 585–595.
- Sussarellu, R., Suquet, M., Thomas, Y., Lambert, C., Fabioux, C., Pernet, M.E.J., Goïc, N.L., Quillien, V., Mingant, C., Epelboin, Y., Corporeau, C., Guyomarch, J., Robbens, J., Paul-Pont, I., Soufant, P., Huvet, A., 2016. Oyster reproduction is affected by exposure to polystyrene microplastics. P. Natl. Acad. Sci. USA 113, 2430–2435.
- Tagg, A.S., Harrison, J.P., Ju-Nam, Y., Sapp, M., Bradley, E.L., Sinclair, C.J., Ojeda, J.J., 2017. Fenton's reagent for the rapid and efficient isolation of microplastics from wastewater. Chem. Commun. 53, 372–375.
- Teng, J., Wang, Q., Ran, W., Wu, D., Liu, Y., Sun, S., Liu, H., Cao, R., Zhao, J., 2019. Microplastic in cultured oysters from different coastal areas of China. Sci. Total Environ. 653, 1282–1292.
- Thompson, R., Olsen, Y., Mitchell, R., Davis, A., Rowland, S.J., John, A.W.G., McGonigle, D., Russell, A.E., 2004. Lost at sea: where is all the plastic? Science 304, 838.
- Van Alstyne, K.L., Nelson, T.A., Ridgway, R.L., 2015. Environmental chemistry and chemical ecology of "green tide" seaweed blooms. Integr. Comp. Biol. 55, 518–532.
- Veerasingam, S., Saha, M., Suneel, V., Vethamony, P., Rodrigues, A.C., Bhattacharyya, S., Naik, B.G., 2016. Characteristics, seasonal distribution and surface degradation features of microplastic pellets along the Goa coast, India. Chemosphere 159, 496–505.
- Wang, J., Liu, X., Liu, G., Zhang, Z., Wu, H., Cui, B., Bai, J., Zhang, W., 2019a. Size effect of polystyrene microplastics on sorption of phenanthrene and nitrobenzene. Ecotox. Environ. Safe. 173, 331–338.
- Wang, W., Gao, H., Jin, S., Li, R., Na, G., 2019b. The ecotoxicological effects of microplastics on aquatic food web, from primary producer to human: a review. Ecotox. Environ. Safe. 173, 110–117.
- Wang, T., Zou, X., Li, B., Yao, Y., Zeng, Z., Li, Y., Yu, W., Wang, W., 2019c. Preliminary study of the source apportionment and diversity of microplastics: taking floating microplastics in the South China Sea as an example. Environ. Pollut. 245, 965–974.
- Xu, D., Schaum, C.E., Lin, F., Sun, K., Munroe, J.R., Zhang, X., Fan, X., Teng, L., Wang, Y., Zhuang, Z., Ye, N., 2017. Acclimation of bloom-forming and perennial seaweeds to elevated pCO₂ conserved across levels of environmental complexity. Global Change Biol. 23, 4828–4839.
- Yang, L., Li, K., Cui, S., Kang, Y., An, L., Lei, K., 2019. Removal of microplastics in municipal sewage from China's largest water reclamation plant. Water Res. 155, 175–181.
- Ye, N., Zhang, X., Mao, Y., Liang, C., Xu, D., Zou, J., Zhuang, Z., Wang, Q., 2011. 'Green tides' are overwhelming the coastline of our blue planet: taking the world's largest example. Ecol. Res. 26, 477–485.
- You, C., Zeng, F., Wang, S., Li, Y., 2014a. Preference of the herbivorous marine teleost *Siganus canaliculatus* for different macroalgae. J. Ocean Univ. China 13, 516–522.
- You, C., Zeng, F., Wang, S., Li, Y., 2014b. Preference of the herbivorous marine teleost *Siganus canaliculatus* for different macroalgae. J. Ocean Univ. China 13, 516–522.
- Yue, F., Gao, G., Ma, J., Wu, H., Li, X., Xu, J., 2019. Future CO₂-induced seawater acidification mediates the physiological performance of a green alga *Ulva linza* in different photoperiods. PeerJ 7, e7048.
- Zhang, J., Huo, Y., Yu, K., Chen, Q., He, Q., Han, W., Chen, L., Cao, J., Shi, D., He, P., 2013a. Growth characteristics and reproductive capability of green tide algae in Rudong coast, China. J. Appl. Phycol. 25, 795–803.
- Zhang, J., Huo, Y., Zhang, Z., Yu, K., He, Q., Zhang, L., Yang, L., Xu, R., He, P., 2013b. Variations of morphology and photosynthetic performances of *Ulva prolifera* during the whole green tide blooming process in the Yellow Sea. Mar. Environ. Res. 92, 35–42.
- Zhang, C., Jeong, C.B., Lee, J.S., Wang, D., Wang, M., 2019a. Transgenerational proteome plasticity in resilience of a marine copepod in response to environmentally relevant concentrations of microplastics. Environ. Sci. Technol. 53, 8426–8436.
- Zhang, Y., He, P., Li, H., Li, G., Liu, J., Jiao, F., Zhang, J., Huo, Y., Shi, X., Su, R., 2019b. *Ulva prolifera* green tide outbreaks and their environmental impact in the Yellow Sea, China. Natl. Sci. Rev. 6, 825–838.
- Zhao, J., Ran, W., Teng, J., Liu, Y., Liu, H., Yin, X., Cao, R., Wang, Q., 2018. Microplastic pollution in sediments from the Bohai Sea and the Yellow Sea. China. Sci. Total Environ. 640, 637–645.
- Zhu, L., Bai, H., Chen, B., Sun, X., Qu, K., Xia, B., 2018. Microplastic pollution in North Yellow Sea, China: observations on occurrence, distribution and identification. Sci. Total Environ. 636, 20–29.